The correlation between the active/buried faults and aeromagnetic data in inner and inner-east Anatolia, Turkey

Ezgi Erbek-Kiran[*,1], Abdullah Ates[2], Mustafa Nuri Dolmaz[1]

[(1)] Suleyman Demirel University, Faculty of Engineering and Natural Sciences, Department of Geophysical Engineering, 32260, Isparta, Turkey
[(2)] Ankara University, Faculty of Engineering, Department of Geophysical Engineering, 06100, Besevler, Ankara, Turkey

Abstract

The paper focuses on investigating the active/buried faults in inner and inner-east Anatolia, Turkey based on aeromagnetic data and comparison with the active fault map. This region includes the major tectonic units of Turkey and the largest basins of Turkey (Tuzgölü Basin (TB) and Sivas Basin (SB)). Thus, the region deserves a detail investigation to delineate the lineaments of the active/buried fault system or the causative sources located in the upper crust. To this end, the region has been divided into two parts as region-1 and 2 including TB and SB, respectively. In this context, the geophysical data processing techniques including power spectrum analysis, high-pass filter, and second vertical derivative method (SVD) have been applied to the aeromagnetic data of the both regions. Firstly, by utilizing power spectrum analysis, the average depths of the deep and shallow causative sources in the region-1 have been calculated as 11.37 km and 5.01 km whereas those depths are 8.5 km and 3.24 km for region-2. Afterwards, to enhance the responses of the residual anomalies, the high-pass filter and the SVD method have been applied to the data. Hereby, these potential lineaments produced from the SVD map have been compared with the active fault map to delineate the uncovering buried faults and their lineaments in the region. Contrary to the discussion in the literature, this study revealed for the first time that the Tuzgölü fault zone located in the eastern part of lake does not merge with the Ecemis fault (EF) zone. Furthermore, the study has shown that this fault zone extended from Kayseri city to Sivas city does not junction with North Anatolian Fault Zone in the north, as well.

Keywords: Aeromagnetic data; Derivative method; Inner Anatolia; Fault

1. Introduction

The convergence and collision movements between the African/Arabian and Eurasian continents evolved the Anatolian microplate. The Anatolia includes large crystalline complexes (massifs) such as Menderes massif and the Central Anatolia Crystalline Complex (CACC). The study area shown by a rectangle on the tectonic map, which

is an object of this study, covers the major part of the CACC (Fig. 1a). The CACC was formed by the closure of the Neotethyan Ocean during the late Mesozoic-Cenozoic. It has a triangular shape that is bounded by major tectonic structures: the Izmir-Ankara-Erzincan suture zone in the north, the Inner Tauride suture zone in the east, the right-lateral strike-slip Tuzgölü fault [Gorur et al., 1998] in the west and the Tauride (I-T) in the south. Also, the CACC is considered to be a microcontinent in the Alpine-Himalayan belt including the high-grade metamorphic rocks (southeast of Ankara), ophiolites (with upper Mesozoic age to the north, north-west, and north-east of the CACC), mafic magmatic rocks, Pliocene volcanic rocks (along the south-east part of the CACC), and Miocene-Pliocene metasediments [Ketin, 1966; Sengor and Yilmaz, 1981]. On the other hand, this continental collision between the African-Arabian and Eurasian plates had an impact on the development of the Neogene and Quaternary volcanism of Central Anatolia. One of these volcanic regions, which is the central part of the Central Anatolian Volcanic Province, is Cappadocian Volcanic Complex (CVC). This volcanic province is located in the transcurrent fault systems known as Tuzgölü and Central Anatolia Fault Zone (CAFZ) (Fig.1a) and it is composed of the volcano-sedimentary units, cinder cones, and volcano-clastic units including the Upper Miocene-Holocene ignimbrites [Innocenti et al., 1975; Pasquare et al., 1988; Froger et al., 1998]. The other volcanic province is Neogene-Quaternary Niğde Volcanic Complex (NVC) located in the western part of the CVC region. The region contains Miocene-Pliocene volcanic rocks, late Neogene-Quaternary polygenetic volcanos, Quaternary domes, and fluvial deposits.

Due to the tectonic regime in the region, many fault systems have developed. The Tuzgölü Fault Zone (TGFZ), for instance, is one the most important tectonic structures that extends NW-SE direction in the region. It is a dextral strike-slip fault and its length of approximately 220 km [Kocyigit and Beyhan, 1998]. This fault zone is known as the Şereflikoçhisar-Aksaray fault in the literature. Also, it is divided into two major branches: the Sultanhanı-Gölören fault in the south (SGF) and the Sülüklü-Cihanbeyli fault (SCF) in the north [Aydemir and Ates, 2006a]. In addition, Tuzgölü Basin (TB), which is the largest interior basin located in Central Anatolia, is located in the south of the lake and is defined as a fault-controlled basin [Aydemir and Ates, 2006a, b]. The surface of this basin is generally covered by the Neogene and Quaternary sediments while the southern part of the basin is covered by the CVC. On the other hand, it is surrounded by the Kırşehir metamorphic units, metamorphic units of the Menderes-Taurus Platform, and ophiolitic and mafic-ultramafic units in the east, west, and north directions, respectively. The other important basin in the region is the Haymana Basin (HB) related to Tuzgölü Basin. These two basins are separated from each other by the Tersakan Basin that has channel-shaped [Aydemir, 2005]. Similar to the Tuzgölü Basin, this basin is also covered with Neogene and Quaternary sediment units. In addition, ophiolitic and mafic-ultramafic units and outcrops (the so-called Karakaya complex) are located in the northern part of the basin. In addition to these, one of the largest basins in Central Anatolia, Turkey is the Sivas Basin. This basin is located in the easternmost of the Kırşehir Block (innereast Turkey) and it is 250 km long and 50 km wide and it was formed resulting from the collisional movement in within a Late Cretaceous-early Tertiary. On the other hand, the basin can be evaluated into two sections: the western and the eastern parts. The reason for this division can be associated with the developing post-collisional deformation since the mid-Miocene times [Buyuksarac, 2007]. The western part of the basin (SW of Sivas) is extended in NE-SW while the eastern part of the basin is oriented in E-W direction (Fig. 1a). The basin has sedimentary fill including the products of magmatic activity [Poisson et al., 1996]. Ophiolitic rocks outcrop located in the northern and southern boundary of the basin are considered as part of the southern Pontide accretionary complex and the products of the Inner Tauride Ocean, respectively [Gansser, 1974; Sengor ve Yilmaz, 1981].

Many studies have been carried out by researchers for this region in order to reveal the geological properties and tectonic structure. However, there is still limited study carried out through potential field data. Some of these geophysical studies are summarized as follows; Ates et al. [1999] constituted the gravity and aeromagnetic anomaly map of Turkey including the current study area. Ates et al. [2005] plotted the Curie point depth map of Central Anatolia using magnetic data and they calculated the Curie point depths ranging from 7.9 to 22.6 km. Aydemir and Ates [2005] investigated the evolution of Central Anatolian basin using the gravity and magnetic data. After, they interpreted the Sülüklü-Cihanbeyli-Gölören magnetic anomalies in the region [Aydemir and Ates, 2006a]. As well, they identified the structure of the Haymana and Tuzgölü Basins [Aydemir and Ates, 2006b]. Onal et al. [2008] investigated the deep structure of the Sivas Basin through gravity and seismic data. They constituted the 3D model of the basin and calculated the deepest part of the basin as 13 km. Aydemir [2009] studied the tectonic development of the Central Anatolia and constituted the tectonic model for the region. Buyuksarac et al. [2005] showed the rotational effect inner East Anatolia and they revealed that there is a good consistence between magnetic anomalies and anticlockwise rotations. In addition, they calculated the top and bottom depths of the volcanic rocks on the
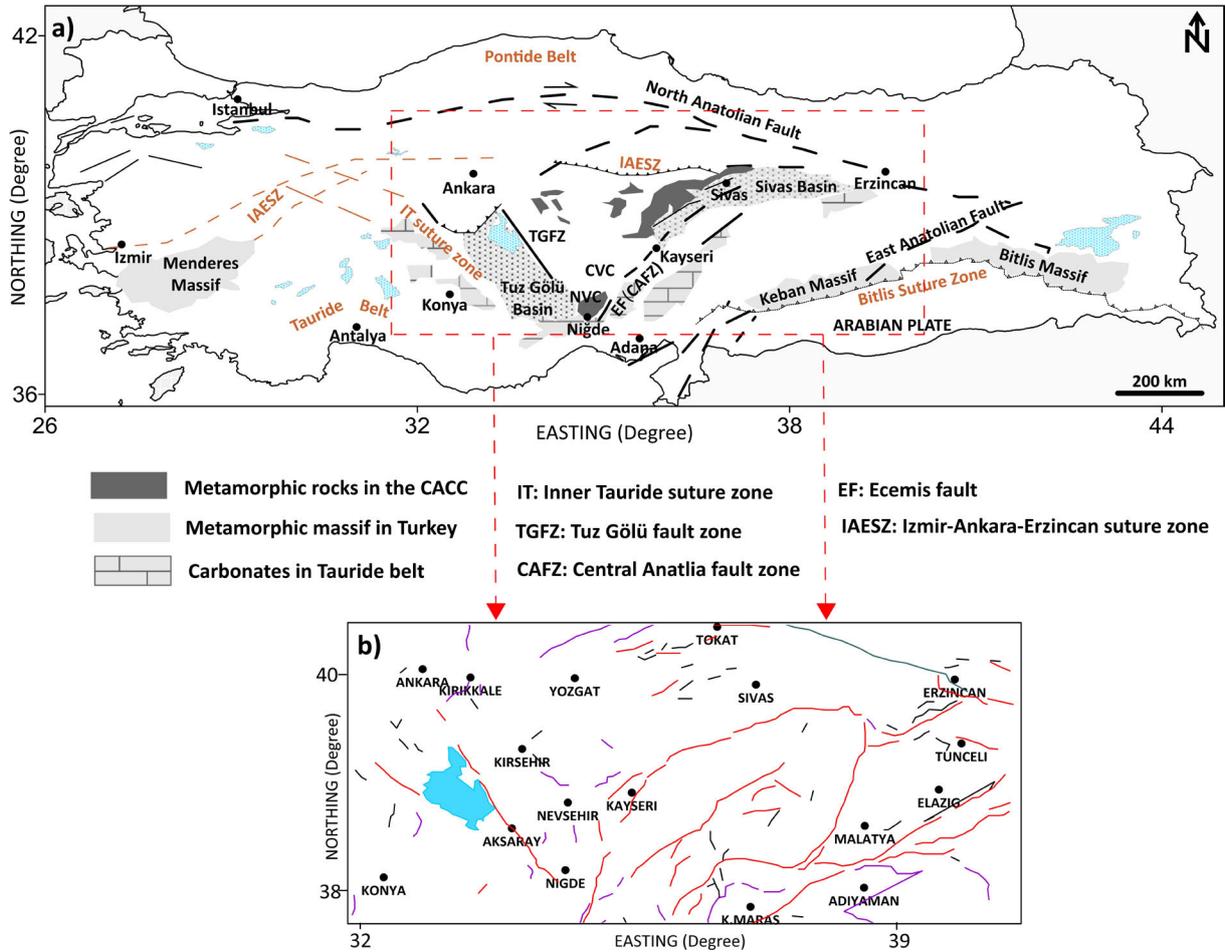
Figure 1. a) Simplified tectonic units and major lineaments in the Turkey (modified from Gursoy et al., [2003]). b) Active fault map of the region (Modified from 1/1250000 digital active fault map of Mineral Research and Exploration General Directorate of the Republic of Turkey, Emre et al., [2013]). Red colour: Holocene fault, Purple colour: Quaternary fault.)

surface as 4 km and 5.7 km, respectively. They implied that the deep magnetized body could be a source of volcanic activity in the region. After this study, Buyuksarac [2007] carried out the regional wrench tectonics of inner East Anatolia through potential field data. Aydemir [2011] investigated the hydrocarbon potential in the Haymana Basin, Central Anatolia and prepared the 3D depth model. Kosaroglu et al. [2016] modelled the shallow structures in the CVP using the gravity and aeromagnetic data. They defined the bottom depth and the top depth of the shallow causative bodies as 2 km and 0.3 km, respectively. Bilim et al. [2017] examined the thermal structure of the Cappadocia region and constituted the Curie point depth and heat flow maps.

As can be seen from the studies abovementioned studies, the outcomes on the linearities of the fault zones in the region are quite limited. In the literature, some arguments have still continued about the conjunction of these fault zone around Niğde city. Similarly, it is important to investigate whether the faults in the vicinity of Sivas city are also merged with the NAFZ. To contribute those gaps, this study focuses on revealing the extensions of faults in the region through magnetic data and comparing them to the current active fault map (Fig. 1b) constituted by Emre et al. [2013]. Briefly, revealing the trace and extension of these fault zones has become a requirement for geophysics. One way to define these faults is to apply the potential field data processing techniques. Henceforth, this research paper is organized as follows: after a brief description of the geological and tectonic background of the region in the introduction section, a description of the data used in the present study will be given in section 2. Section 3 covers the advanced potential field techniques (power spectrum analysis, high-pass filter, and second vertical derivative methods) applied to these data. Also, it presents the maps and their interpretation of them obtained from these techniques. Finally, section 4 concludes the paper.

2. Aeromagnetic data

Aeromagnetic data processed in this study are provided from the General Directorate of the Mineral Research and Exploration Company of Turkey (MTA). The measurement was taken at an elevation of 600 m above the surface along N-S trending profiles. In addition, the International Geomagnetic Reference Field [IGRF 1982.5] correction, which is one of the magnetic correction methods, was applied to this dataset for reduction. After the required corrections, the dataset is gridded with a sampling interval of 10 km. The other technical information about the dataset was given by Ates et al. [1999]. The aeromagnetic anomaly map of Central Anatolia, Turkey, which has been re-created in this study is given in Figure 2. As can be seen from the figure, the study area has been divided into two parts: region-1 and region-2. These regions shown in the blue box are enlarged and the dataset has been gridded with a sampling interval of 2.5 km (Figs. 3a and 3b).
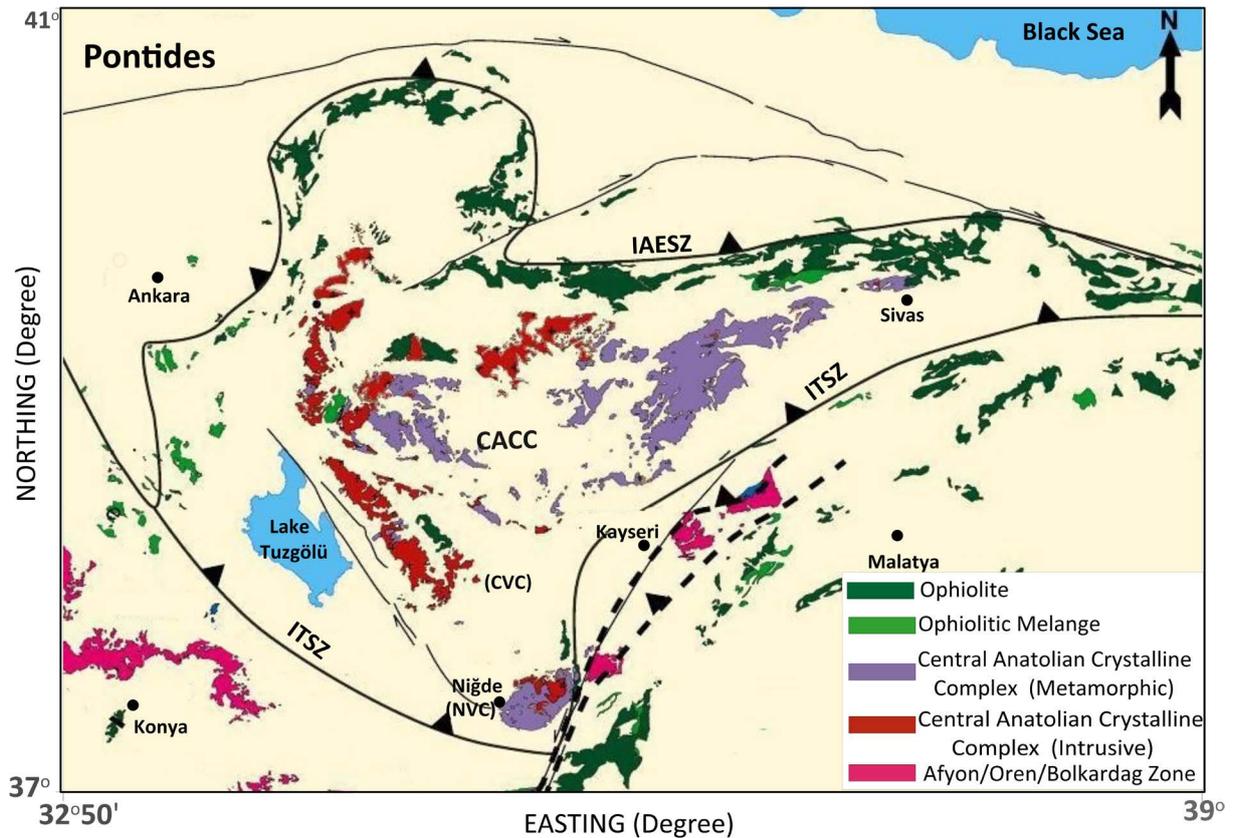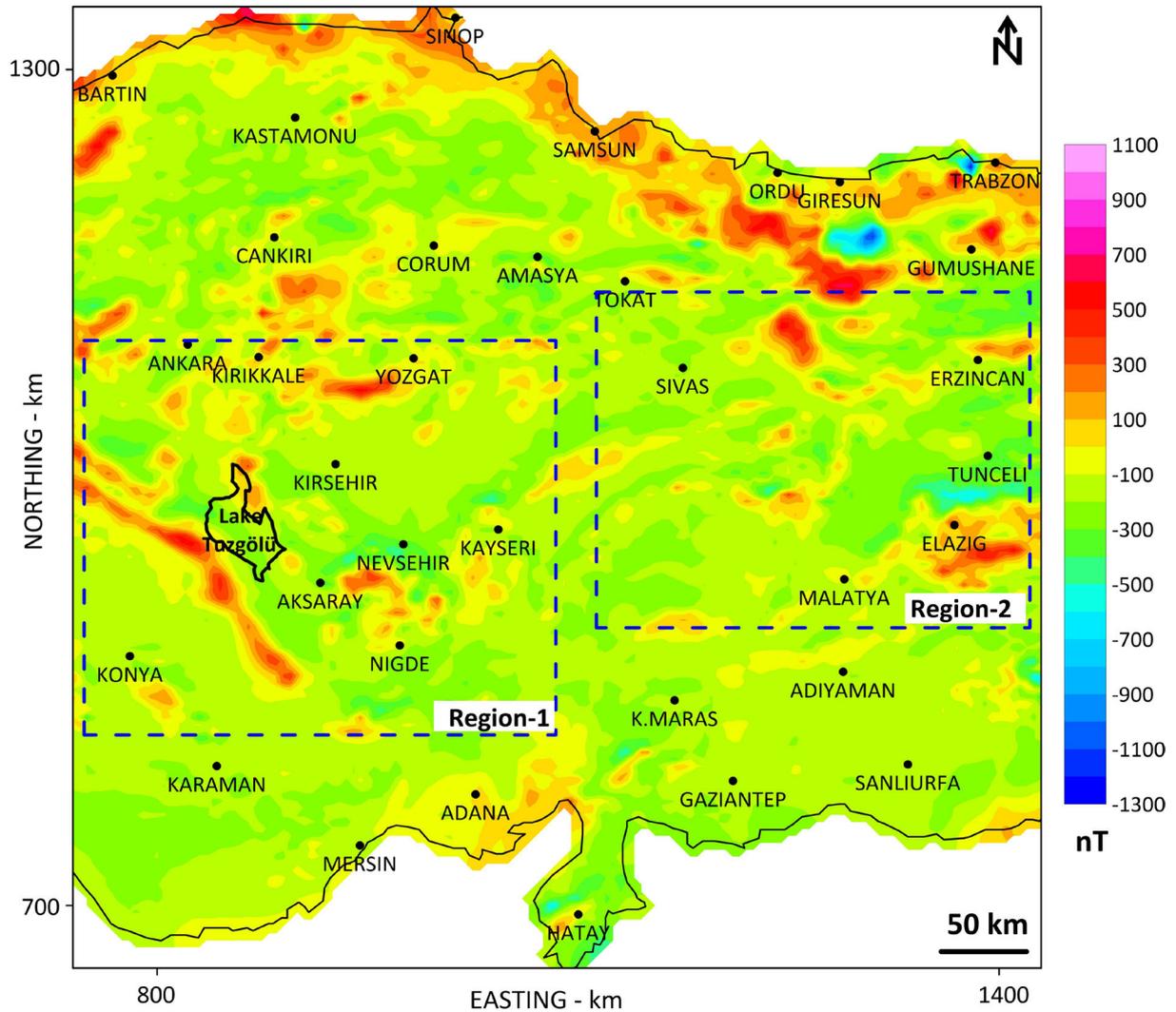

Figure 2. The aeromagnetic anomaly map of the Central Anatolia, Turkey.

Figure 3a shows that the region-1 has the aeromagnetic anomaly values vary between -1000 and +1000 nt and the traces of the major structure in the region such as TGFZ, EF (CAFZ), and I-T suture zone are clearly observed in this map. The anomalies of the SCF and SGF are seen as a linear magnetic anomaly in the NW-SE direction. Another anomaly located on the northern part of Lake Tuzgölü could be evaluated as the Deliler anomaly named for the first time by Aydemir [2005]. It is considered that this anomaly is caused by the volcanic mass under the surface [Aydemir, 2005]. The other intense magnetic anomaly located in the southernmost of Yozgat city takes attention. This anomaly trending E-W direction could be associated with the granitoid assemble and ophiolites in the region. Also, the Cappadocian Volcanic Complex (CVC) between Aksaray, Niğde, and Nevşehir city formed above the metamorphic basement of the CACC displays intense aeromagnetic anomalies, as well (Fig. 3a). Figure 3b shows the distribution of the aeromagnetic anomaly map of the region-2. By a closer look at Figure 3b, it is observed that the high intensity magnetic anomalies located in the SE of the Sivas City correspond to the plutonic rocks in the region and the iron mine. The other anomaly located between Sivas and Erzincan Cities is the largest magnetic anomaly in the region.

The existence of the anomaly could be associated with the ophiolitic rock assemblages in the northern part of the region and plutonic rocks. On the other hand, low magnetic anomaly values have been observed in the Sivas Basin (located in the SE of Sivas City). The detailed geology map is given in previous studies [Ates et al., 2005 for region-1; Bilgic, 2002 for region-2]. Therefore, it is not repeated in this paper. However, considering these geology maps, it could be said that the magnetic anomalies are in harmony with the surface geology of both regions.

Figure 3. a) The aeromagnetic anomaly map of the region-1. HB: Haymana Basin, TB: Tuzgölü Basin, SCF: Sülüklü-Cihanbeyli fault, SGF: Sultanhanı-Gölören fault b) The aeromagnetic anomaly map of the region-2. SB: Sivas Basin.

In order to follow the traces of these fault zones in detail, it has been deemed appropriate to apply some advanced potential field data techniques. Thus, it will be possible to determine whether these fault zones converge near the Niğde city. These techniques are summarized in the next section.

3. Geophysical methods and interpretation

3.1 Radially averaged power spectrum

Power spectrum analysis has been widely used in potential field data processing. As well-known, potential field data contains two anomaly components; regional and residual anomalies. Residual anomalies caused by shallower

magnetized bodies are often suppressed by regional anomalies caused by deeper magnetized bodies. Therefore, the estimation of the depth of these magnetized bodies could be a difficult issue. Applying the power spectrum analysis developed by Spector and Grant [1970], the average depth of the magnetized bodies could be easily estimated. In this study, power spectrum analysis has been applied to aeromagnetic data, and logarithmic power spectrum values have been plotted versus the wavenumber. The average depths of the magnetized objects have been calculated from the slope of the lines through the points on the graph (Depth $= -\dfrac{\text{Slope}}{4\pi}$). The average depth of the deep magnetized bodies in the region-1, whose frequencies range from 0.003 to 0.04 cycle/km, has been calculated as 11.37 km while the average depth of the shallow magnetized bodies, whose frequencies range from 0.004 to 0.10 cycle/km, has been calculated as 5.01 km. In addition, the cut-off frequency (fc) value obtained from the graph is determined to be 0.046 cycle/km (Fig. 4a). With the application of this technique to the region-2, the average depth of the deep magnetized bodies is calculated as 8.5 km while the average depth of the shallower sources is calculated as 3.24 km. The cut-off frequency is also determined to be 0. 072 cycles/km (Fig. 4b).
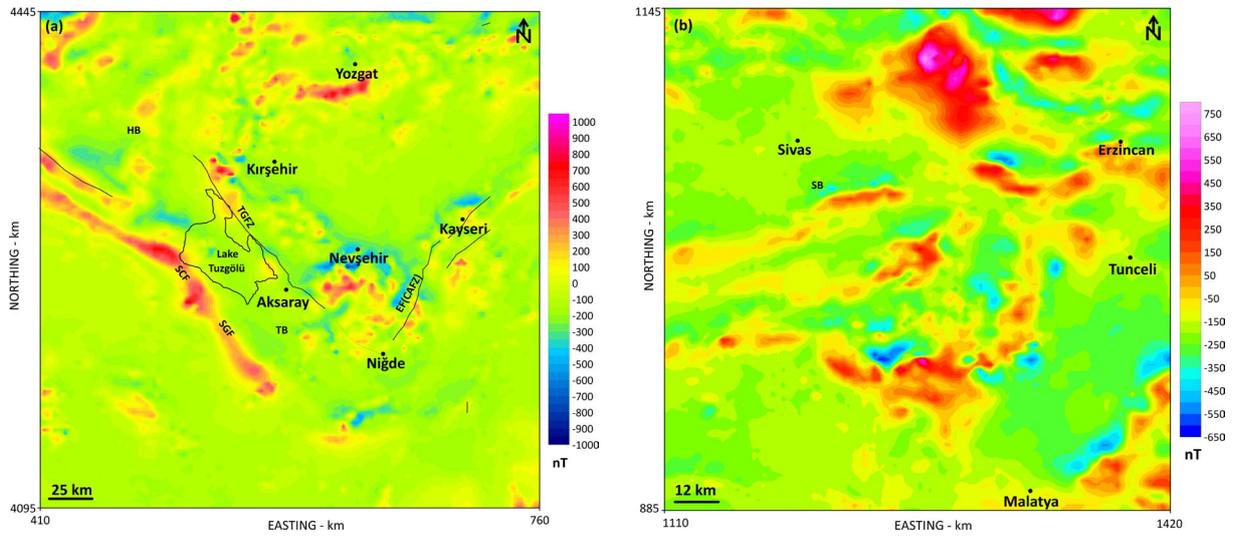

Figure 4. a) Radially averaged power spectrum of the region-1. b) Radially averaged power spectrum of the region-2.

3.2 High-pass filtering anomalies

A high-pass filter is one of the ways to make clear the effects caused by the shallow bodies in the anomaly maps in geophysical investigations. In other words, the effects caused by deep causative bodies have been removed from the total aeromagnetic data via this filter and the short-wavelength/high-frequency components caused by the shallow bodies in the total aeromagnetic data have been emphasized.

In this study, the high-pass filter has been applied to the aeromagnetic anomalies using the cut-off frequency of 0.046– for the region-1. Hereby, the residual anomalies caused by the shallow bodies are made clear on the map. The high-pass filtered map is given in Figure 5a. According to the map, the positive anomalies in the west and NE direction of Lake Tuzgölü have been observed. These anomalies could be associated with the arc-related granitoid. Also, the linear anomaly named as Sülüklü-Cihanbeyli-Gölören anomaly by Aydemir and Ates [2006a] has been clearly observed on the map. This anomaly with the NW-SE direction extends along the western boundary of the Lake.

The cut-off frequency for the region-2 has been obtained from the power spectrum analysis as 0.072 cycle/km. Hereby, with the application of the high pass filter, the effects caused by the shallow magnetized bodies have been enhanced on the map (Fig. 5b). The high magnetic intensities in the NE of Sivas city could be associated with the existence of the ophiolitic unit considering the surface geology in the region and the metamorphic basement. As can be seen from the resulting maps, the filtering process has provided a big advantage to emphasize the effects of shallow sources. Besides these, the negative or low intensity aeromagnetic anomalies observed in the Sivas Basin are probably caused by the existence of sedimentary units including Lower to Mid-Miocene evaporitic rocks.
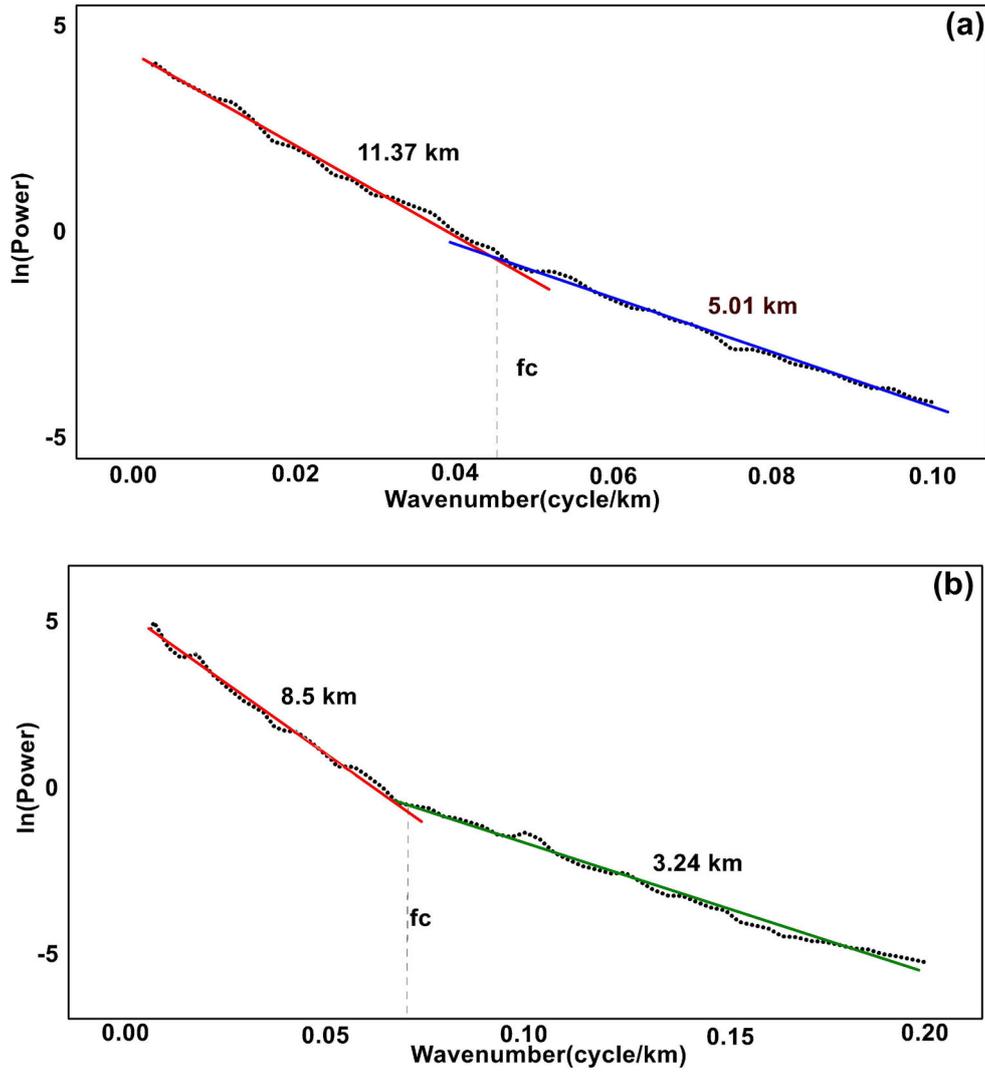
Figure 5. a) High-pass filter anomaly map of the region-1. b) High-pass filter anomaly map of the region-2.

3.3 Second vertical derivative (SVD)

Derivative methods are widely used to make clear the boundaries of the causative source in the anomaly maps. Hereby, it becomes easier to understand the effects caused by shallow sources in the interpretation process. In other words, the application of this method provides a better view for us to delineate the near-surface features in the maps. Moreover, the SVD method gives very effective results, especially in revealing geological structures such as normal or reverse faults. The method developed by Blakely [1995] using the Fourier transform is formulated as:

$$F = \left[\frac{\partial^n P}{\partial Z^n}\right] = |k|^n F|P| \tag{1}$$

where P is the potential field data, k is the wavenumbers, and n is the degree of vertical derivative. In this study, we have applied the SVD methods to the filtered data for both regions and created the SVD anomaly maps (Figs. 6a and 6b). Hereby, the effects of shallow bodies and their geometries have been enhanced in the maps. By a closer look at Figure 6a, a remarkable anomaly with NW-SE trending has been observed in the western bound of Lake Tuzgölü. It is noteworthy that this anomaly including the SCF and SGF zones and their extensions of these fault zones have been seen clearly. Similarly, the anomaly located between Niğde and Kayseri city extends in NE-SW direction. It could be said that this anomaly corresponds to the EF (CAFZ) (Fig. 1a). On the other hand, there is no

junction/meeting point around Niğde city (Fig. 6a). In other words, it is revealed that the TGFZ (Fig. 1a) located in the eastern part of Lake Tuzgölü does not junction with the EF (CAFZ) zone in this study, contrary to the discussion [Coskun, 2004] in the literature. According to Fig. 6b, the Sivas Basin does not include any magnetized body creating a remarkable anomaly while the boundaries of the causative sources located around the basin have been observed clearly. The reason for not observing the magnetic anomalies in the basin could be explained as that the basin is filled with non-magnetic units. In addition, the anomalies caused by ophiolite and plutonic rocks are located in the northern part of the map. Furthermore, it could be thought that the anomalies located in the SVD map are consistent with the active fault map (Fig. 1b) given by Emre et al. [2013].
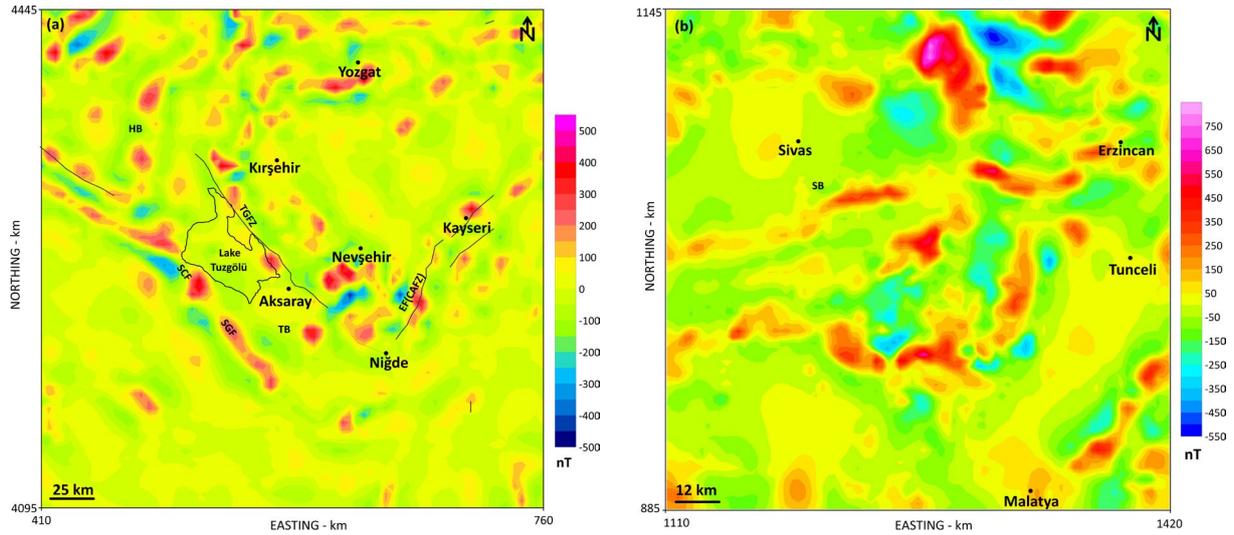
Figure 6. a) The SVD map of the aeromagnetic data for region-1. b) The SVD map of the aeromagnetic data for region-2. The regions shown by the blue-coloured dashed lines are defined as the fault zones.

4. Conclusion

This paper has presented the correlation between the active buried faults and aeromagnetic data in inner and inner-east Anatolia, Turkey based on the aeromagnetic data and analysis of these data. As mentioned before, the region includes two major basins in Central Anatolia, Turkey and it is bounded by the crucial tectonic lineaments. On the other hand, the only major tectonic unit in the region that can be observed on the surface is TGFZ. Thus, the region requires more research in terms of revealing the buried fault and trace of the lineaments. In this study, for the first time, the lineaments in the upper crustal structure have been revealed and they have correlated with the active fault map constituted utilizing the surface geology. In accordance with this purpose, the study region has been divided into two parts; region-1 and region-2, and the aeromagnetic data for both regions have been processed by using advanced potential field data. In doing so, we focus on emphasizing the effects of the residual anomalies caused by shallower sources. Besides, it is worth mentioning that reduced-to-pole transformation has not been executed to these data due to severe remnant magnetization in the region. Firstly, power spectrum analysis has been applied to the aeromagnetic data in order to determine the average depths of the causative/magnetized bodies. By using this technique, the average depths of the shallower and deeper magnetized bodies for both regions have been calculated. The average depth of the causative bodies (shallow and deep) for region-1 have been computed as 5.01 km and 11.37 km, respectively (Fig. 4a) while these depths for region-2 have been computed as 3.24 km and 8.5 km (Fig. 4b). From here on in, to emphasize the effects of the shallower sources, the cut-off frequencies have been obtained by using the graph plotted the logarithmic power spectrum versus wavenumber. In this way, the cut-off frequencies obtained from here allow to application of the high-pass filter for both regions. With the application of the filter, the anomalies caused by the deep magnetized bodies have been surpassed while the anomalies caused by the shallow magnetized bodies have been made clearer in both regions. Finally, the SVD method has been applied to the data in order to distinguish the effects caused by regional and residual anomalies. The reason for applying

this method can be expressed as the effects of small-scale causative bodies are often suppressed by the effects of regional anomalies and the anomalies of small bodies could be concealed on the map. By doing so, the responses of the small and shallow sources in the study regions have been accentuated on the map. Also, the comparison of the SVD map for region-1 (Fig. 6a) and the active fault map (Fig. 1b) has observed some differences. For instance, the active fault map does not include the SCF and SGF zones determined in the previous study by Aydemir (2005) while the trace of these fault zones has been observed clearly on the SVD map in the current study. In other words, it could be expressed that the method gives successful results in revealing the lineaments of the fault based on this example. Similarly, the lineaments of EF (CAFZ) (Fig. 1a) extending NE-SW direction have been observed on the map, as well. Furthermore, this study has shown that there is no junction between the EF (CAFZ) zone and TGFZ based on the lineaments on the SVD map. In addition, it is seen that the anomalies on the map are concentrated around the city of Nevşehir. These anomalies correspond to the Cappadocia region that occupies a vast area in the eastern part of Aksaray city. Eruptive volcanics in the region cover a major part of the surface. Thus, it is considered that these anomalies could be associated with these volcanics. On the other hand, the anomalies located in the western boundary of Lake Tuzgölü look like C-shape (including Yozgat, Kırşehir and Nevşehir city). These anomalies could be considered that it is related to the magmatic arc (Kırşehir – mentioned by Gogus et al. 2017) including arc-related granitoid units. Similarly, when the SVD map of region-2 has been compared to the active fault map, it has been observed that there are some consistencies in each other. For instance, the lineaments of the EAFZ extending the NE-SW direction (south of Sivas city) have been seen clearly on the SVD map (Fig. 6b). Also, lineaments that constituted the boundary of the Sivas Basin have been revealed in the current study (marked with a blue lines). Especially, the lineament located in the bottom boundary of the basin is consistent with the fault given in the active fault map. Thus, it could be reasonable to say that this lineament could be a continuation of EF (CAFZ) and this continuation has been revealed by using aeromagnetic data for the first time. On the other hand, the lineament extending the N-W direction in the centre of the map (marked with blue lines) takes attention. It is thought that these anomalies may indicate a fault structure that is observed in the active fault map given in Fig. 1b. Furthermore, the study has shown that this fault zone does not junction with NAFZ in the north, as well. The lineaments located in the north of Sivas City could be seen prominently on the SVD map (Fig. 6b – blue lines in the north) and these anomalies correspond to the Izmir-Ankara-Erzincan suture zone and ophiolitic mélange located in this suture zone. As a conclusion, image maps with high resolution have been obtained from the current study to determine the lineaments and the findings compare the active fault map. It is possible to say that the lineaments determined by the current study deserve further investigation in the future.

References

Ates, A., F. Bilim and A. Buyuksarac (2005). Curie Point Depth Investigation of Central Anatolia, Turkey, Pure Appl. Geophys., 162, 357-371.

Ates, A., P. Kearey and S. Tufan (1999). New gravity and magnetic anomaly maps of Turkey, Geophys. J. Int., 136, 499-502.

Aydemir, A. (2005). Investigation of structural geology and hydrocarbon potential of the Tuzgölü Basin and surrounding area by using geophysical methods (Unpublished PhD thesis), Ankara University, Turkey (in Turkish with English abstract).

Aydemir, A. (2009). Tectonic investigation of Central Anatolia, Turkey, using geophysical data, Journal of Applied Geophysics, 68, 321-334.

Aydemir, A. (2011). An integrated geophysical investigation of Haymana Basin and hydrocarbon prospective Kirkkavak Formation in Central Anatolia, Turkey, Petroleum Geoscience, 17 (1), 91-100. doi: https://doi.org/10.1144/1354-079310-004

Aydemir, A. and A. Ates (2005). Preliminary evaluation of Central Anatolian Basins in Turkey using the gravity and magnetic data, Journal of Balkan Geophysical Society, 8, 7-19.

Aydemir, A. and A. Ates (2006a). Structural interpretation of the Tuzgolu and Haymana Basins, Central Anatolia, Turkey, using seismic, gravity and aeromagnetic data, Earth, Planets and Space, 58, 951-961.

Aydemir, A. and A. Ates (2006b). Interpretation of Suluklu-Cihanbeyli-Goloren Magnetic Anomaly, Central Anatolia, Turkey: an integration of geophysical data, Phys. Earth Planet. Inter., 159, 167-182.

Bilgic, T. (2002). Geological Map of Turkey (1:500.000 Scale Sivas sheet), General Directorate of Mineral Research and Exploration. (MTA), Ankara.

Bilim, F., S. Kosaroglu, A. Aydemir and A. Buyuksarac (2017a). Thermal investigation in the Cappadocia Region, Central Anatolia-Turkey, analyzing the Curie Point Depth, Geothermal Gradient and Heat Flow maps from the aeromagnetic data, Pure Appl. Geophys., 147, 4445-4458.

Blakely, R.J. (1995). Potential theory in gravity and magnetic applications, Cambridge University Press, NY, USA, pp 441.

Buyuksarac, A. (2007). Investigation into the regional wrench tectonics of inner East Anatolia (Turkey) using potential field data. Phys. Earth Planet. Inter., 160, 86-95.

Buyuksarac, A., D. Jordanova, A. Ates, and V. Karloukovski (2005). Interpretation of the gravity and magnetic anomalies of the Cappadocia Region, Central Turkey, Pure Appl. Geophys., 162, 2197-2213.

Coskun, B. (2004). Aksaray and Ecemis Faults-Diapiric Salt Relationships: relevance to the hydrocarbon exploration in the Tuz Golu (Salt Lake) Basin, Central Anatolia, Turkey. Energy Sources 26, 1005-1022

Emre, O, T.Y. Duman, S. Ozalp, H. Elmaci, S. Olgun and F. Saroglu (2013). Active fault map of Turkey with an Explanatory Text. 1/1,250,000 scale, General Directorate of Mineral Research and Exploration, Special Publication Series-30, Ankara-Turkey. ISBN: 978-605-5310-56-1 https://www.mta.gov.tr/en/maps/active-fault-1250000

Froger, J.L., J.F. Lenat, J. Chrowicz, J.L. Le Pennec, J.L. Bourdier, O. Kose, O. Zimitoglu, N.M. Gundogdu and A. Gourgaud (1998). Hidden calderas evidenced by multisource geophysical data; example of Cappadocian Calderas, Central Anatolia, J. Volcanol. Geoth. Res., 185, 99-128.

Gansser, A. (1974). The ophiolitic melange, a worldwide problem on Tethyan examples, Eclog. Geol. Helv., 67, 479-507.

Gogus, O.H., R.N. Pysklywec, A.M.C. Sengor and E. Gun (2017). Drip tectonics and the enigmatic uplift of the Central Anatolian Plateau, Nat. Commun., 8, 1538.

Gorur, N., O. Tuysuz and A.M.C. Sengor (1998). Tectonic evolution of the Central Anatolian Basins, Int. Geol. Rev., 40, 831-850.

Gursoy, H., J.D.A. Piper and O. Tatar (2003). Neotectonic deformation in the western sector of tectonic escape in Anatolia: palaeomagnetic study of the Afyon region, central Turkey, Tectonophysics 374, 57-79.

Innocenti, F., G. Mazzuoli, F. Pasquare, F. Radicati Di Brozolo and L. Villari (1975). The Neogene calcalkaline volcanism Central Anatolia: geochronological data on Kayseri-Nigde area, Geol. Mag., 112, 349-360.

Kocyigit, A. and A. Beyhan (1998). A new intra-continental transcurrent structure; the Central Anatolian Fault Zone, Turkey, Tectonophysics, 284, 317-336.

Ketin, I. (1966). Tectonic units of Turkey, Mineral Research and Technical Institute Bulletin 66, 20-34 [in Turkish].

Kosaroglu, S., A. Buyuksarac and A. Aydemir (2016). Modeling of shallow structures in the Cappadocia region using gravity and aeromagnetic anomalies, J. Asian Earth Sci., 124, 214-226.

Onal, K.M., A. Buyuksarac, A. Aydemir and A. Ates (2008). Investigation of the deep structure of the Sivas Basin (innereast Anatolia, Turkey) with geophysical methods, Tectonophysics, 460, 186-197.

Pasquare, G., S. Poli, L. Vezzoli and A. Zanchi (1988). Continental arc volcanism and tectonic setting in Central Anatolia, Turkey, Tectonophysics, 146, 217-230.

Poisson, A.M., J.C. Guezou, A. Ozturk, S. Inan, H. Temiz, H. Gursoy, K.S. Kavak and S. Özden (1996). Tectonic Setting and Evolution of the Sivas Basin, Central Anatolia, Turkey,. Int. Geol. Rev., 38(9), 838-853.

Sengor, A.M.C. and Y. Yilmaz (1981). Tethyan evolution of Turkey: a plate tectonic approach, Tectonophysics, 75, 181-241.

Spector, A. and F.S. Grant (1970). Statistical models for interpreting aeromagnetic data, Geophysics, 35, 293-302.

*CORRESPONDING AUTHOR: Ezgi ERBEK-KIRAN

Suleyman Demirel University, Faculty of Engineering and Natural Sciences, Department of Geophysical Engineering Isparta, Turkey

ezgierbek@sdu.edu.tr